Transmitter Concentration Profiles in the Synaptic Cleft: An Analytical Model of Release and Diffusion

J. Kleinle,* K. Vogt,# H.-R. Lüscher,# L. Müller,* W. Senn,* K. Wyler,* and J. Streit#
#Physiologisches Institut and *Institut für Informatik und angewandte Mathematik, Universität Bern, CH-3012 Bern

ABSTRACT A three-dimensional model for release and diffusion of glutamate in the synaptic cleft was developed and solved analytically. The model consists of a source function describing transmitter release from the vesicle and a diffusion function describing the spread of transmitter in the cleft. Concentration profiles of transmitter at the postsynaptic side were calculated for different transmitter concentrations in a vesicle, release scenarios, and diffusion coefficients. From the concentration profiles the receptor occupancy could be determined using α-amino-3-hydroxy-5-methyl-4-isoxazolepropionic acid receptor kinetics. It turned out that saturation of receptors and sufficiently fast currents could only be obtained if the diffusion coefficient was one order of magnitude lower than generally assumed, and if the postsynaptic receptors formed clusters with a diameter of roughly 100 nm directly opposite the release sites. Under these circumstances the gradient of the transmitter concentration at the postsynaptic membrane outside the receptor clusters was steep, with minimal cross-talk among neighboring receptor clusters. These findings suggest that for each release site a corresponding receptor aggregate exists, subdividing an individual synapse into independent functional subunits without the need for specific lateral diffusion barriers.

INTRODUCTION

The original model of quantal synaptic transmission at the neuromuscular junction suggested that quantal size is determined by the amount of transmitter released from one vesicle (Del Calstillo and Katz, 1954). More recently it has been proposed that quantal size at central synapses is determined by the size of the postsynaptic receptor cluster sitting opposite the release site (Redman, 1990). This hypothesis requires a transmitter concentration that saturates the receptors. There is now additional evidence for a saturation of receptors during synaptic transmission, based on the effects of competitive antagonists to *N*-methyl-D-aspartate (NMDA) receptors (Clements et al., 1992; Tang et al., 1994). However, two recent observations are difficult to reconcile with the hypothesis of receptor saturation. First, it has been shown that even at single synaptic terminals, miniature currents attributed to the spontaneous release of transmitter from single vesicles show a large variation in amplitude (Bekkers et al., 1990; Liu and Tsien, 1995; Vogt et al., 1995). This variation is difficult to explain with the hypothesis that all miniature currents are determined by receptor saturation. Second, recent evidence for multivesicular release would constitute a redundant mechanism if receptors are saturated by the transmitter released from a single vesicle (Tong and Jahr, 1994). We have recently reported that the currents induced by the exposure of glutamate to single synapses are much larger in amplitude than quantal synaptic currents originating from identical sites, suggesting that only a fraction of the receptors are occupied during quantal release (Vogt et al., 1995). On the other hand, we showed in the same publication that nonstationary variance analysis of quantal currents was best interpreted in terms of receptor saturation. These conflicting results lead us to suggest that postsynaptic receptors may form several independently operating subclusters opposite single terminals. To evaluate whether this model would hold in the absence of any lateral diffusion barriers between subclusters of receptors, we tried to estimate the size of the postsynaptic membrane patch exposed to saturating concentrations of transmitter originating from a single vesicle. We show that the problem can be solved analytically. The results suggest that saturation of postsynaptic receptors can only be achieved if the diffusion coefficient of glutamate in the synaptic cleft is one order of magnitude lower than generally assumed (cf. Wathey et al., 1979; Bartol et al., 1991; Holmes, 1995) and if the postsynaptic receptors form clusters with a radius of 50–100 nm opposite release sites. Under these circumstances the concentration profile of transmitter at the postsynaptic side is such that several release sites may operate independently of each other at one synaptic terminal.

Model

General framework of the model

The distribution of transmitter in the synaptic cleft after the release of a vesicle depends on a number of parameters: the time course of release of transmitter from the vesicle, the diffusion coefficient in the synaptic cleft, the geometrical configuration of the synaptic cleft, the binding of transmitter to the postsynaptic receptors or reuptake transporters, and the eventual breakdown of transmitter in the cleft. For many of these parameters we lack precise experimental data. Recent attempts have been made to describe the re-

Received for publication 15 March 1996 and in final form 20 July 1996.
Address reprint requests to Dr. J. Kleinle, Institut für Informatik und angewandte Mathematik, Universitat Bern, Neubruckstrasse 10, CH-3012 Bern, Switzerland. Tel.: 41-31-631-3403; Fax: 41-31-631-3965; E-mail: kleinle@iam.unibe.ch.

0006-3495/96/11/2413/14 $2.00

lease process (e.g. Bruns and Jahn, 1995) and the spread of transmitter in the synaptic cleft for central and peripheral synapses (Clements et al., 1992; Colquhoun et al., 1992; Barbour et al., 1994). All models (Wathey et al., 1979; Busch and Sakmann, 1990; Bartol et al., 1991; Faber et al., 1992; Holmes, 1995; Wahl et al., 1996) are based on instantaneous release. (The model of Wahl et al. (1996) was extended, taking into account the release of transmitter from a spherical vesicle driven by diffusion.) Recent experimental evidence from cultured leech neurons (Bruns and Jahn, 1995) suggests that this is probably not a realistic assumption. Therefore we used an approach where the model could be used for any instantaneous and continuous release functions.

Outline

The following framework was defined for the analysis. The released transmitter propagates freely across the cleft according to the diffusion equation. The treatment of the diffusion process is presented in the next section. The assumptions presented above allow a fully analytical description and lead to a solution of the three-dimensional diffusion equation with a continuous source term. The diffusion process is treated first to point out that it is independent of any choice of parameters (diffusion coefficient, source function). For details about the derivation of the solution we refer the interested reader to the Appendix. The parameters are specified, beginning with the geometry of the synaptic structure and the concentration of transmitter in the vesicle (see Transmitter Release, below). The transmitter is released from a single vesicle according to the real-time measurement done by Bruns and Jahn (1995). The geometrical parameters of the synaptic structure and the concentration of transmitter in the vesicle were chosen as described by Clements et al. (1992) (Transmitter Release). Ultrastructural evidence (cf. Fig. 1) suggests that the synaptic cleft is shaped like a flat cylinder (cf. Fig. 2 *A*). The calculated concentration of transmitter at the postsynaptic side was used to simulate the current flow through postsynaptic receptors, based on the kinetics of α-amino-3-hydroxy-5-methyl-4-isoxazolepropionic acid (AMPA) receptors (Jonas et al., 1993) (see Kinetic Model, below). The transmitter bound to the receptors was neglected for the calculation of the concentration profiles.

Diffusion across the synaptic cleft

The average movement of transmitter particles inside the cleft obeys diffusion dynamics. The propagation of the concentration profiles is described mathematically by an inhomogeneous three-dimensional diffusion equation (Eq. 1). The inhomogeneity is given by the release source. The presented solution is valid for any release source. The differential equation is transformed into an integral, which is simpler to interpret and numerically evaluable with arbitrary accuracy. The boundary conditions of the synaptic cleft are then introduced. The mathematical approach is briefly outlined in this section; the details are summarized in the Appendix.

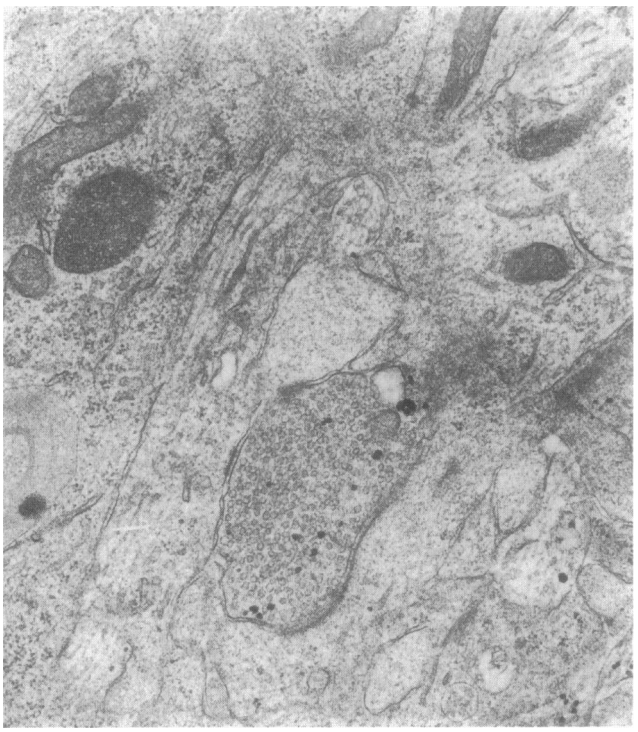

FIGURE 1 Ultrastructural evidence for several release sites in one synaptic terminal. Electromicrograph of a synaptic terminal in a slice culture of the rat spinal cord (14 days in vitro). (magnification ×22,600). Two well-separated narrow active zones can be seen at the upper side of the terminal, whereas one long active zone seems to be present at the lower side.

Diffusion with a source is described by an inhomogeneous differential equation with fixed initial value,

$$\frac{\partial}{\partial t} n(x, y, z, t) = D\left(\frac{\partial^2}{\partial x^2} + \frac{\partial^2}{\partial y^2} + \frac{\partial^2}{\partial z^2}\right) n(x, y, z, t) + f(x, y, z, t), \quad (1)$$

where $f(x, y, z, t)$ is the source and $n(x, y, z, t)$ is the density of transmitter in the cleft. (If instantaneous release without further source is assumed, the mathematical formulation would be a homogeneous differential equation with a fixed initial value; cf. Eq. 6.) D is the diffusion coefficient. The initial value (closed vesicle) is given by $n(x, y, z, 0) = 0$. For the moment, free boundaries at infinity are chosen in the x, y, and z directions. This partial differential equation is solved by the method of Green's function. The derivation of the solution in free space is presented in the Appendix (Diffusion with Source Term). In the synaptic cleft, the transmitter is reflected at the pre- and postsynaptic sides. To satisfy the boundary conditions of the cleft (cf. Eq. 11), one

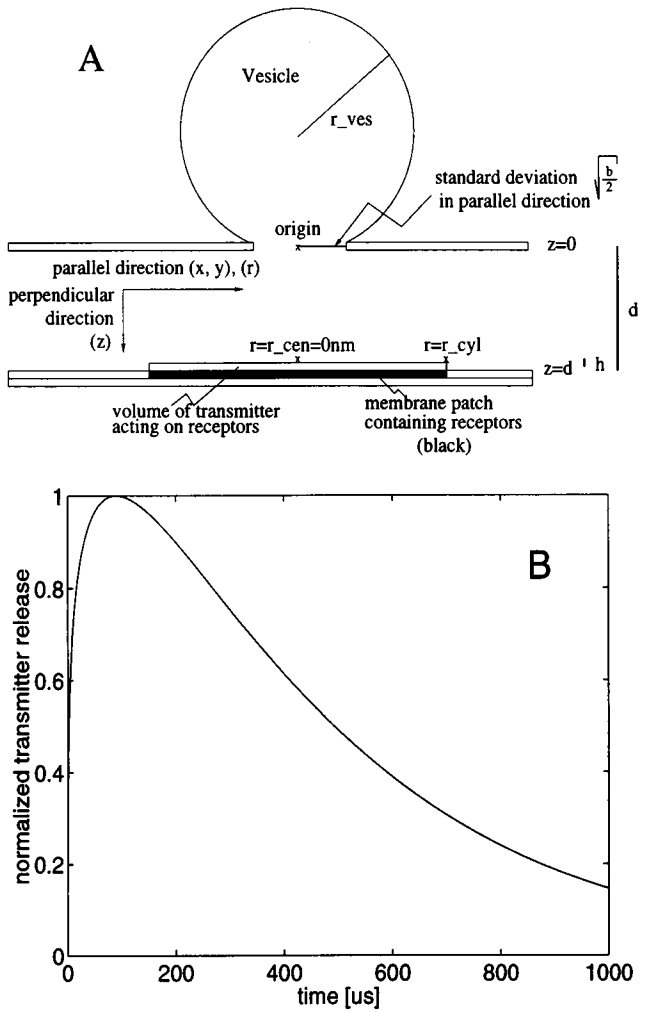

FIGURE 2 (*A*) Schematic drawing of the geometrical configuration of the model synapse. z is the perpendicular (vertical) and r (rsp. x, y) the parallel variable. The origin is the center of the vesicle pore. r_{ves} is the vesicle radius. The standard deviation $\sqrt{b/2}$ of the source function in the parallel direction is shown in the vesicle pore. The cleft width is d, the height of the cylinder containing transmitter acting on the receptors is h. The circular membrane patch containing receptors with radius r ($r_{cen} = 0$ nm $< r < r_{cyl}$) is black. (*B*) Time course of transmitter release. Cf. Eq. 3 (Bruns and Jahn, 1995).

makes use of the method of reflection (for details see Appendix, Diffusion in the Synaptic Cleft). One superposes an infinite chain of solutions of Eq. 1 corresponding to transmitter release at sites $z = 2jd$ for all integers j, where d is the cleft width. This leads to the transmitter density in the synaptic cleft,

$$n(x, y, z, t) = \sum_{j=-\infty}^{\infty} \int_0^t \int_{-\infty}^{\infty} \int_{-\infty}^{\infty} \int_{-\infty}^{\infty} f(\xi, \upsilon, \zeta, \tau) \left(\frac{1}{4\pi D(t-\tau)}\right)^{3/2} \exp\left\{-\frac{(\xi - x)^2 + (\upsilon - y)^2 + (\zeta - (z - 2jd))^2}{4D(t-\tau)}\right\} d\xi d\upsilon d\zeta d\tau. \quad (2)$$

Specifying the source function $f(x, y, z, t)$, the density of transmitter particles at every position (x, y, z) in the cleft and every moment t can be calculated using Eq. 2.

Transmitter release

Transmitter release from one vesicle (Bruns and Jahn, 1995) is described by the source function

$$f(x, y, z, t) = q \cdot g(x, y, z) t^{\alpha} \exp\{-\beta t\}, \quad (3)$$

with a Gaussian $g(x, y, z)$ in the x, y, and z directions, centered at the origin, given by

$$g(x, y, z) = \exp\left\{-\frac{x^2 + y^2}{b} - \frac{z^2}{c}\right\}. \quad (4)$$

$b/2$ are variances in x, y, and $c/2$ in the z direction; $q > 0$ is a normalization factor; and $t^{\alpha}\exp\{-\beta t\}$ is an α-type function in time. (The initial variance in the $x-$,y-direction is limited by the lateral size of the release pore. The variance in the z direction is at least smaller than the cleft width. The geometrical configuration of the model is depicted in Fig. 2 *A*. The numerical value of b and c (1×10^{-4} $(\mu m)^2$) turned out to be of minor importance. The diffusion dynamics is ruled by the term $(4Dt + b)^{3/2}$. For the used range of the diffusion coefficient D and time t we have $b/Dt \ll 1$ (the same argument can be applied to c (cf. Fig. 6).) $f(x, y, z, t)$ defines the transmitter flow through the vesicle pore into the synaptic cleft. The time course of transmitter release at the vesicle pore is shown in Fig. 2 *B*. Because we are interested in the neurotransmitter glutamate, we refer to estimates given by Clements et al. (1992) for the initial concentration in the vesicle and the geometrical configuration (values given for central synapses). A concentration of 100 mM inside the vesicle (diameter 40 nm) corresponds to ~2000 molecules.

Inserting into Eq. 2 the source function $f(x, y, z, t)$ as given in Eq. 3, the space integrals are solvable (for details see the Appendix, Diffusion in the Synaptic Cleft). Integrating over the space variables in Eq. 2, the density $n(x, y, z, t)$ of transmitter in the cleft is given by

$$n(r, z, t) = \frac{qb\sqrt{c}}{4D} \sum_{j=-\infty}^{\infty} \int_0^{4Dt} \frac{(t - (s/4D))^{\alpha} \exp\{-\beta(t - (s/4D))\}}{\sqrt{c + s}(b + s)} \exp\left\{-\frac{r^2}{b + s} - \frac{(z - 2jd)^2}{c + s}\right\} ds. \quad (5)$$

Numerical values of the parameters are listed in Table 1. x and y are replaced by the radial distance r. The boundary conditions ensure that all released transmitter is diffusing inside the synaptic cleft. However, the integral cannot be solved analytically. One has to evaluate the integral numerically. But we successfully reduced the computation of four integrals in Eq. 2 to only one in Eq. 5. The integration of Eq. 5 was done by Mathematica (Wolfram Research, 1994), which uses an adaptive algorithm for one-dimensional integration, subdividing the integration region recursively.

TABLE 1 Parameter values and ranges

Name	Symbol	Value	Unit	Reference
Glutamate molecules per vesicle	Q	$(1 - 4) \cdot 10^3$	molecules	Clements et al. (1992)
Glutamate concentration in the vesicle	c_0	(60–200)	mM	Clements et al. (1992)
Vesicle radius	r_{ves}	20	nm	Clements et al. (1992)
Cleft width	d	20	nm	Clements et al. (1992)
Release rise time	t_{rise}	90	(μs)	Bruns and Jahn (1995)
Release decay time constant	β	1/360	1/(μs)	Bruns and Jahn (1995)
$t_{rise} \cdot \beta$	α	1/4	—	Bruns and Jahn (1995)
Diffusion coefficient of glutamine in water	D	$7.6 \cdot 10^{-6}$	cm^2/s	Longsworth (1953)

TABLE 2 Transition rates

k^*_{AB}	k^*_{BC}	k^*_{DE}	Unit	k_{CO}	k_{OC}	k_{CB}	k_{BA}	Unit	k_{BD}	k_{DB}	k_{CE}	k_{EC}	k_{OF}	k_{FO}	k_{ED}	k_{EF}	k_{FE}	Unit
50.5	24.1	2.54	$mM^{-1}ms^{-1}$	14.84	1.9	6.8	119.3	ms^{-1}	1.16	0.12	0.08	7.e-3	0.46	4.e-3	0.046	0.017	0.1904	ms^{-1}

The transition rates given in set 1 by Jonas et al. (1993) were multiplied by the following factors to produce the values given: k^*_{AB}, 11; k^*_{BC}, 0.85; k^*_{DE}, 2; k_{CO}, 3.5; k_{OC}, 2.1; k_{CB}, 2.1; k_{BA}, 28; k_{BD}, 0.4; k_{DB}, 3; k_{CE}, 0.45; k_{EC}, 1; k_{OF}, 28; k_{FO}, 1; k_{ED}, 1; k_{EF}, 1; k_{FE}, 1.

The binary precision of the integrand was 16 bits; the accuracy goal performing the integration was 6 bits. For comparison, alternative release scenarios (instantaneous release and a source emitting at a constant rate) are presented in the Appendix.

Kinetic model

To reconstruct postsynaptic currents and to compare them to experimentally recorded currents, the concentration of transmitter at the postsynaptic membrane has to be calculated. The density of transmitter in the cleft has first to be transformed into postsynaptic concentration (described in the Appendix, Postsynaptic Concentrations). To transform concentrations of glutamate into currents, a kinetic schema of AMPA receptors was used basing on that proposed by Jonas et al. (1993).

The model is briefly outlined in Fig. 3. It comprises an unbounded receptor state (A), a single bound state (B), a double bound state (C), and an open state (O) with their corresponding desensitized states (D, E, and F). The desensitized state (F) is predetermined because the sum of all state probabilities $P(X)$ must equal 1 ($P(F) = 1 - P(A + B + C + D + E + O)$). The transition rates are denoted k_{XY}. X is the label of the initial state and Y of the final state. The set of transition values proposed by Jonas et al. (1993) was adapted to satisfy five constraints: 1) The dose-response curve of the kinetic scheme has to be in reasonable agreement with the dose-response curve of glutamate published by Trussel and Fischbach (1989) for spinal cells. 2) The concentration and time-dependent transition rates have to be in accordance with the range $2\ mM^{-1}ms^{-1} \leq k_{XY} \leq 50\ mM^{-1}ms^{-1}$. 3) k^*_{BC} should be half of k^*_{AB}, to account for the (probable) independent binding of the first and second transmitter molecules to the receptor. 4) The maximum open probability of the receptor should not exceed 80%. 5) The rise time of the miniature currents in spinal slice cultures (Vogt et al., 1995) had to be reproduced. Kinetic schemes obeying these conditions were taken to fit recorded miniature currents. This procedure resulted in the values of Table 2. The forward transition rates (k^*_{AB}, k^*_{BC}, and k^*_{DE}) are concentration and time dependent. The other transition rates are only time dependent. Averaged concentrations, calculated for a circular postsynaptic membrane patch of variable diameter (see Appendix, Postsynaptic Concentrations), were used in assuming clusters of receptors with various diameters. We did not introduce any temperature corrections and refer only to room temperature. The simulation of the receptor kinetics was performed using MATLAB/SIMULINK of the Mathworks. The precision was 3 bits. Calculations with higher precision did not alter the results.

RESULTS

Effects of different release functions on concentration time course

In many previous models, transmitter release has been assumed to take place instantaneously (Wathey et al., 1979; Bartol et al., 1991; Faber et al., 1992; Holmes, 1995). However, experimental data on the time course of release of 5-hydroxytryptamine from cultured leech neurons have been presented recently (Bruns and Jahn, 1995). Our first aim therefore was to test the influence of the release function on the concentration of transmitter in the synaptic cleft. This was possible because the procedure described above (Diffusion Across the Cleft) offers a strategy for finding the analytical solution for any release function. (The function has to obey special boundary and initial conditions (Appendix, Diffusion with Source Term). This is not a physiological restriction.) To compare instantaneous and continuous release, the concentration of transmitter at the postsynaptic side was calculated for different release functions. For instantaneous release, the concentration declined rapidly with

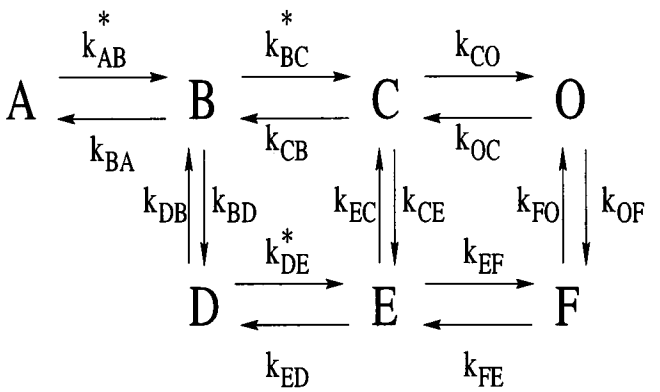

FIGURE 3 Scheme of the receptor kinetics. (A) Unbounded receptor state; (B) a single bound state; (C) double bound state; (O) an open state. The corresponding desensitized states are D, E, F. The transition rates are denoted k_{XY}. X is the label of the initial state and Y of the final. The transition rates marked with stars are time and concentration dependent. The unmarked rates are only time dependent.

time from relatively high values (18 mM; cf. Fig. 4 *A*). The concentration peaked within 1 μs and declined to 10% of its maximum value after 25 μs. No difference was seen in the temporal concentration profile between a Gaussian or a spherical spatial shape of the source (cf. Fig. 4 *A*). In contrast, the concentration of transmitter increased slowly in continuous-release models. The peak concentration at the postsynaptic side was reached only after 250 μs (cf. Figs. 4 *A* and 7 *A*) at a much smaller value (0.37 mM) than was seen for instantaneous release. The concentration declined to 10% of its maximum value after 2 ms. Only a small difference was seen in the concentration time course when an α-shaped release function was compared to a step function source. This finding confirms, first, the correctness of our calculation compared to a well-established analytical approach (Carslaw and Jaeger, 1959). Second, it shows that for poorly defined release functions the approximation by "release histograms" offers an efficient way of estimating the concentration in the cleft. ("Release histograms" approximate the source function at every time step by its time average.) If the diffusion coefficient in the cleft was lowered (see also next section), a higher concentration of transmitter at the postsynaptic side and a slower decay were seen for all release scenarios (Fig. 4 *B*). The concentration declined to 10% of its maximum value 205 μs after instantaneous release. It reached a maximum after 290 μs and declined to 10% of its maximum value after 2.7 ms for continuous release (Fig. 7 *A*). The time course of transmitter in the cleft predicted by the model was used to evaluate the accuracy of the model by comparison to the effects of NMDA antagonists on the time course of NMDA currents in hippocampal cultures (cf. Clements et al., 1992). When the α-shaped release function was used, the time course predicted by the model was much closer to the reported data than that predicted by an instantaneous release model. Therefore, for the remainder of the simulations, release was assumed to follow the experimentally confirmed α-shaped time course.

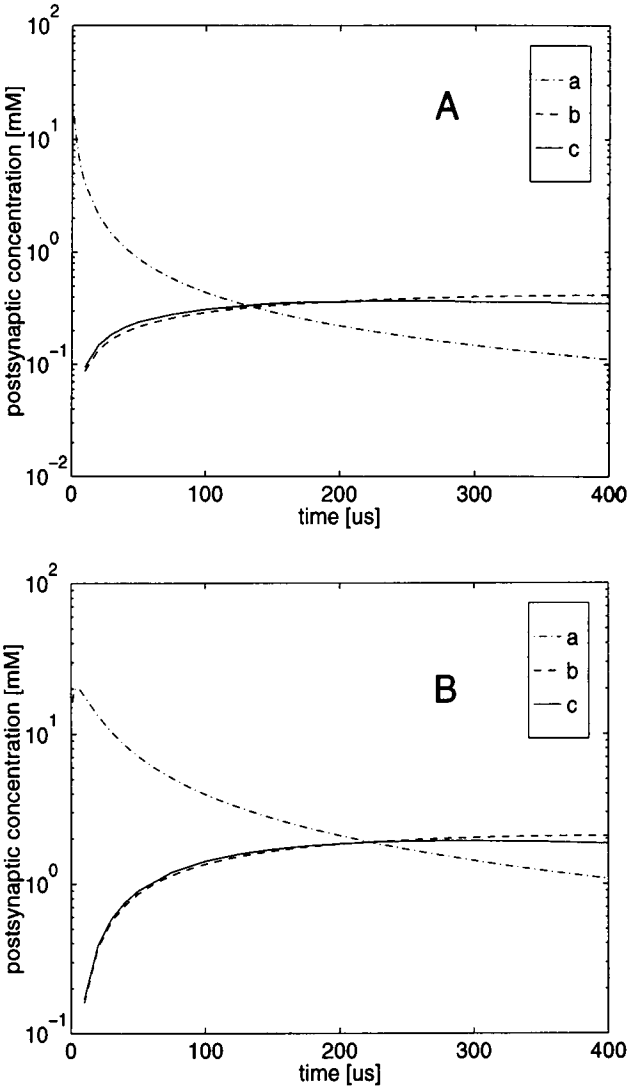

FIGURE 4 Semilogarithmic plots of concentration profiles for instantaneous and continuous release. Chosen parameters: $D = 3 \times 10^{-6}$ cm^2/s, $r = 50$ nm (*A*); $D = 3 \times 10^{-7}$ cm^2/s, $r = 50$ nm (*B*). (a) The concentration profile after instantaneous release. Initial Gaussian (Eq. 7) and initial spherical (Eq. 8) spatial distributions are indistinguishable and drawn in one line. (b and c) The concentration profiles for continuous release. (b) The concentration profile after a source emitting at every time step at a rate corresponding to the time average of Eq. 5 (Eq. 10). (c) The concentration profile after α-shaped release (Eq. 5).

Spatial distribution profiles for different diffusion coefficients

Because the value of the diffusion coefficient (D) of glutamate in the synaptic cleft is unknown, the spatial distribution profiles of transmitter in the cleft were studied for two values of D. The higher value (3×10^{-6} cm^2/s) is usually taken in modeling studies of the diffusion of transmitter in the cleft (Wathey et al., 1979; Busch and Sakmann, 1990; Holmes, 1995). It is 40% of the measured value for glutamine in water at 25°C (7.6×10^{-6} cm^2/s; cf. Longsworth, 1953). The lower value (3×10^{-7} cm^2/s) is 4% of the

measured value for glutamine in water. Lowering D by a factor of 10 had two effects. First, it increased the concentration of transmitter opposite the release site from 0.37 mM to 1.93 mM (after 290 μs; see Figs. 4 and 5). Second, it narrowed the distribution of transmitter in the cleft (Fig. 5). The spatial decay to 10% of the peak transmitter concentration decreased from 300 nm to 120 nm, 200 μs after the onset of release (see Fig. 5, *A* and *B*). However, even for this low value of D, the cleft was crossed by the transmitter within the first tens of microseconds, thus causing an almost uniform distribution along the cleft width (Fig. 6). The continuous release function maintained a high concentration of transmitter opposite the release site (Fig. 5 *A*). This effect was even more pronounced for low values of D, because of a decrease in the lateral dilution of the transmitter (Fig. 5 *B*). For low diffusion coefficients the concentration of transmitter at the postsynaptic membrane was therefore highly dependent on the location relative to the release site (Fig. 5 *D*). For patches located directly opposite the release site, the concentration was high, whereas it rapidly declined for more eccentric patches (for high D see Fig. 5 *C*; for low D see Fig. 5 *D*).

Interaction with receptors and postsynaptic currents

So far no methods exist to measure directly the concentration of transmitter in the synaptic cleft with the necessary spatial and temporal resolution. Indirect experimental ap-

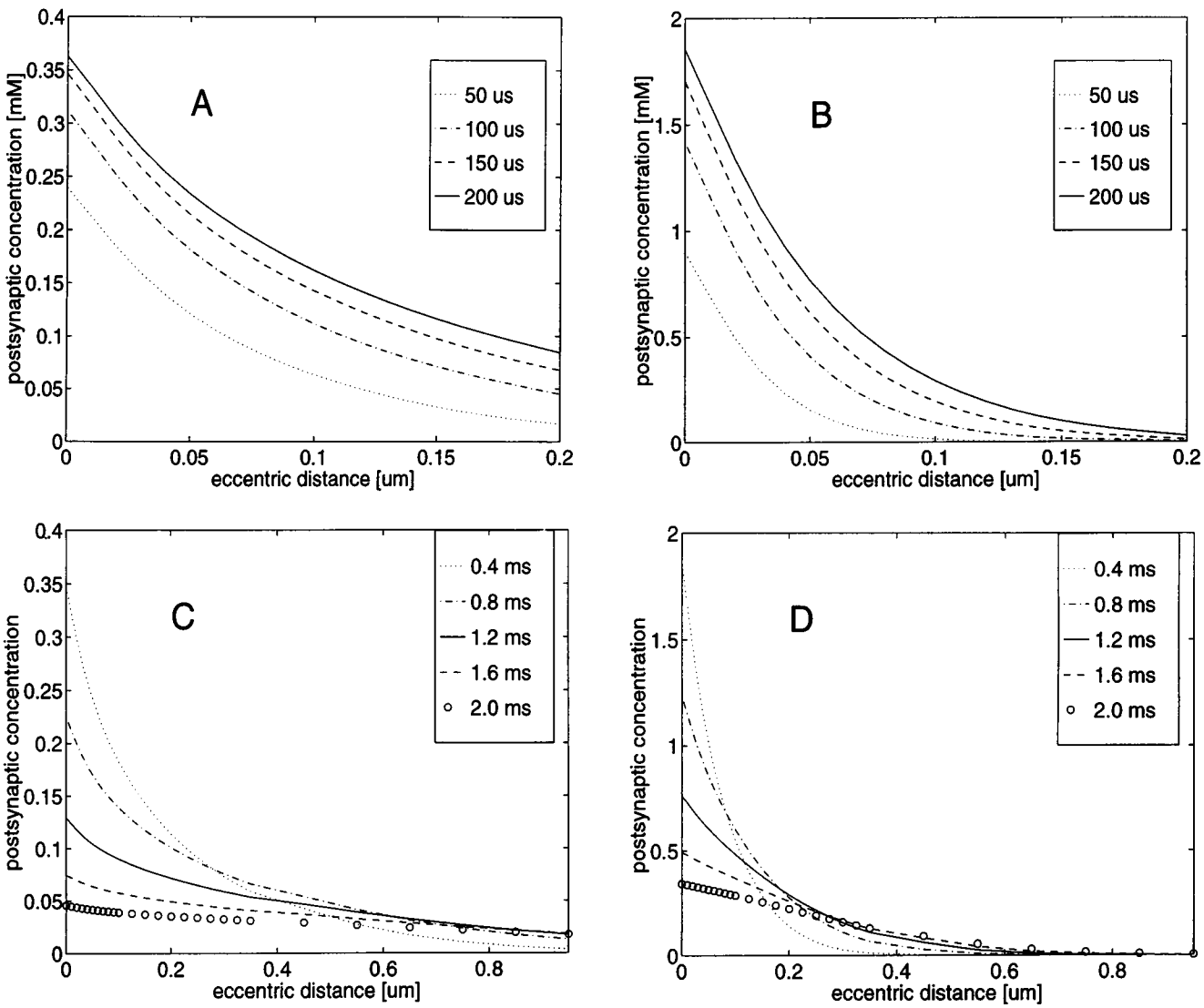

FIGURE 5 Spatial concentration profiles after α-shaped release for different diffusion coefficients. The abscissa is the lateral distance of the patch from the release pore (eccentric distance in μm). The circular membrane patches all have the same radius ($r = r_{cyl} = 50$ nm). (*A*) Spatial concentration profiles for $D = 3 \times 10^{-6}$ cm^2/s, from 50 to 200 μs. (*B*) Spatial concentration profiles for $D = 3 \times 10^{-7}$ cm^2/s, from 50 to 200 μs. (*C*) Extension of *A* to a distance of 950 nm and time 2 ms. (*D*) Extension of *B* to a distance of 950 nm and time 2 ms.

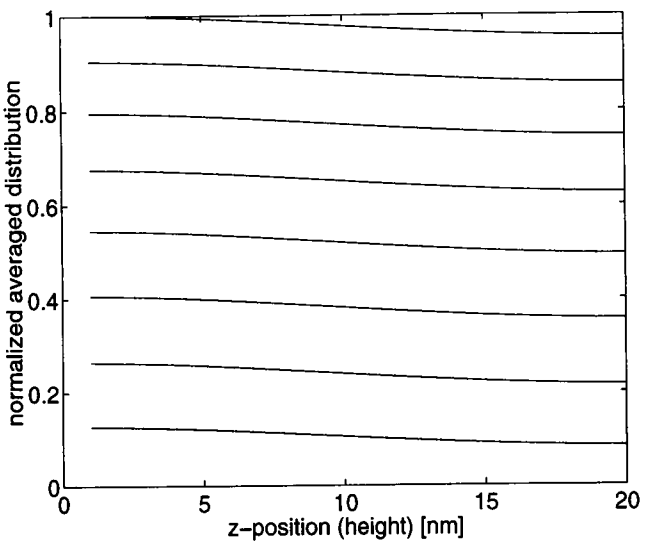

FIGURE 6 Distribution profiles across the cleft. The distribution (averaged over 1 nm of the cleft) of transmitter is plotted versus different z positions for $D = 1 \times 10^{-7}$ cm^2/s. From bottom to top, the transmitter distribution in the cleft is shown from $t = 25$ μs to $t = 200$ μs at 25-μs steps. The negative gradient of each curve shows the extent of inhomogeneity of the distribution over the cleft width. The effect of inhomogeneity is at maximum for the lowest diffusion coefficient ($D = 1 \times 10^{-7}$ cm^2/s). For higher D the transmitter distribution is even more uniform over the cleft.

proaches to synaptic release are based on recordings of postsynaptic currents. To be able to compare the outcome of our simulations to recorded miniature synaptic currents, the calculated concentration of transmitter at the postsynaptic side had to be converted into currents. This was done by using the kinetics of AMPA receptor channels proposed by Jonas et al. (1993) and as described above (Kinetic Model). The model simulates the open probability of the receptor channels for a given transmitter concentration. From the open probability the currents can be calculated using estimated values for the single-channel conductance and the number of receptors (Vogt et al., 1995). To adjust the glutamate sensitivity of the kinetic model to experimental findings, the concentration-dependent transition rates of the model were modulated to fit the dose-response curve reported by Trussel and Fischbach (1989) for spinal neurons (cf. Fig. 7 *C*). The time-dependent transition rates were adjusted to fit the time course of recorded spinal miniature currents (Vogt et al., 1995) (cf. Fig. 7 *B*). This was necessary because the spinal EPSCs are faster than those in hippocampal neurons. The sets of parameters proposed by Jonas et al. predicted currents that were too slow even for a stepwise change to saturating transmitter concentrations. To account for the spatial concentration profiles predicted by the model, the calculations were made for patches of postsynaptic membrane of different diameters under the assumption that the receptors are clustered in these patches (for details see the Appendix, Postsynaptic Concentrations). These patches could be located directly opposite the release sites or eccentric to them. Because neither transmitter concentration in the vesicles nor the diffusion coefficient in the cleft nor the size of the receptor clusters in the postsynaptic membrane is known, open probabilities were calculated for reasonable ranges of these three parameters (see Fig. 8, *B–E*). The results showed that for the high value of D, full saturation of the postsynaptic receptors was not achieved, not even with a transmitter concentration inside the vesicles of 200 mM. Under these circumstances the open probability and therefore the current amplitude are highly dependent on the content of the vesicles, whereas the size of the receptor cluster is less important. For a value of D 10 times lower, the situation was different. Now the size of the receptor cluster became an important factor. For the smallest tested cluster diameter of 100 nm the receptors were practically saturated if the concentration of transmitter in the vesicles was higher than 100 mM. Saturation required a higher transmitter content of the vesicles for larger clusters. In addition, the rise times of the currents were shorter for the lower D values. For eccentric receptor clusters the open probability rapidly decreased with increasing distance from the release site (Fig. 9), because of the steep spatial concentration profiles (Fig. 5, *B* and *D*).

DISCUSSION

General purpose of the study

Quantal models of synaptic transmission have been the object of increasing interest in recent years, mainly because of implications of the models for synaptic plasticity (Kullmann and Nicoll, 1992; Larkman et al., 1991; Malinow and Tsien, 1990). Many conclusions derived from these models are based on indirect results of quantal analysis of postsynaptic potentials or currents, a method whose limitations become more and more evident (Clamann et al., 1991; Dityatev and Clamann, 1993; Isaacson and Walmsley, 1995). To overcome such analytical difficulties, a method has recently been developed to identify synapses on living cells in culture and to stimulate these synapses by iontophoretic application of transmitter (Vogt et al., 1995) or by evoking the release of transmitter at presynaptic boutons (Bekkers et al., 1990; Liu and Tsien, 1995; Vogt et al., 1995). These experiments first showed that the major source of variation in the size of quantal miniature currents is located at single release sites (Bekkers et al., 1990; Liu and Tsien, 1995), and second, that there are many more receptors present at single presynaptic terminals than are saturated by the transmitter released from one vesicle leading to miniature currents (Vogt et al., 1995). These findings are in contrast to reports on the effect of competitive antagonists on postsynaptic currents. The conclusion of the latter experiments was that postsynaptic receptors are almost fully saturated by the transmitter released from single vesicles (Clements et al., 1992; Tang et al., 1994). In a previous report we reached a similar conclusion based on nonstationary variance analysis of miniature currents (Vogt et al.,

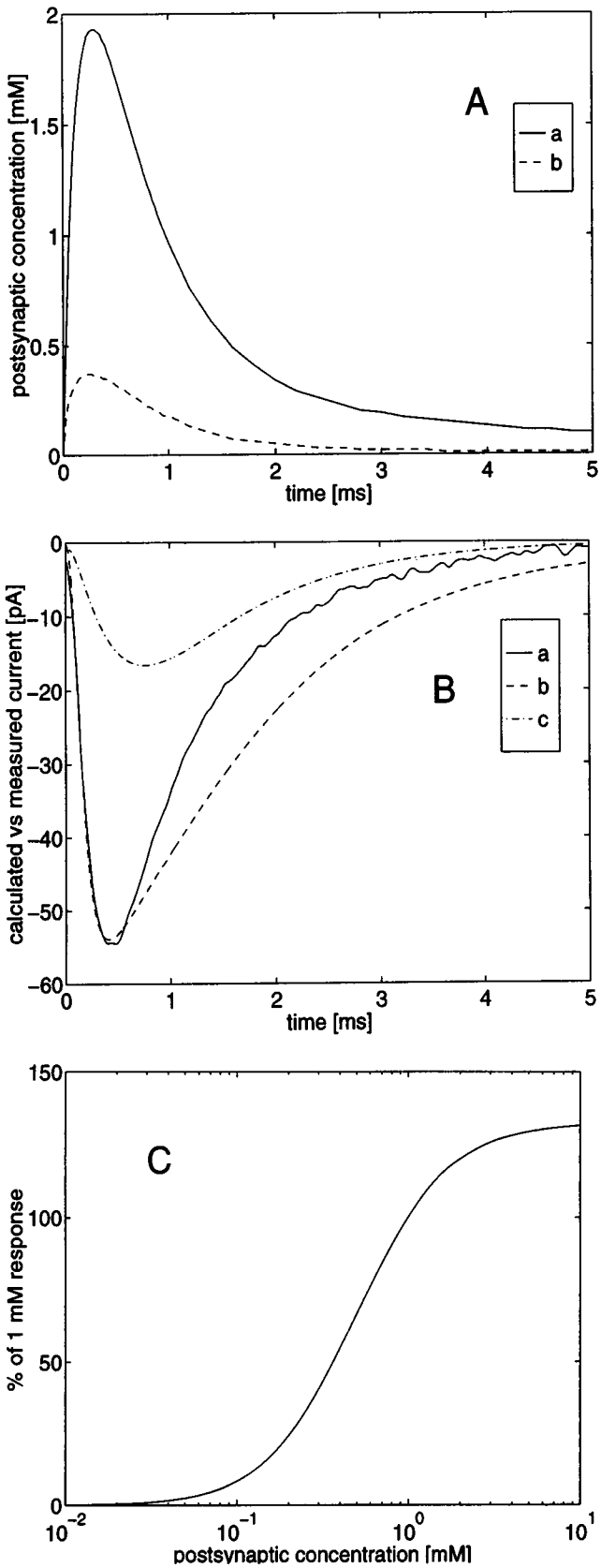

FIGURE 7 Time course of calculated transmitter concentrations and simulated postsynaptic currents compared to recorded miniature currents. (*A*) Postsynaptic transmitter concentrations after α-shaped release versus time for a radius of the receptor field of $r = 50$ nm. (a) $D = 3 \times 10^{-7}$ cm^2/s. (b) $D = 3 \times 10^{-6}$ cm^2/s. (*B*) Simulated postsynaptic currents corresponding to the transmitter concentrations in *A* versus recorded miniature current. (a) Average postsynaptic current from one specific bouton on a rat spinal neuron in culture. The presumed presynaptic terminal was challenged with a brief puff of a high-KCl solution. The subsequent burst of miniature currents was recorded and the individual currents were averaged (cf. Vogt et al., 1995). (b and c) Simulated currents were obtained by applying the concentration shown in *A* to the receptor kinetics and multiplying the resulting channel open probability with $N = 45$ and $i_e = -1.7$ pA. Values for the number N of open channels and single channel current were taken from Vogt et al. (1995). Radius of the receptor field $r = 50$ nm. (b) $D = 3 \times 10^{-7}$ cm^2/s. (c) $D = 3 \times 10^{-6}$ cm^2/s. (*C*) Dose-response curve. Semilogarithmic plot of channel open ratio (response to 1 mM equals 100%) for different constant postsynaptic transmitter concentrations. $P_{max} = 132\%$, Hill coefficient = 1.7, $EC_{50} = 0.49$ mM. This set of parameters is in reasonable agreement with the values for chick spinal neurons given by Trussell and Fischbach (1989) (Hill coefficient = 1.95, $EC_{50} = 0.51$ mM).

1995). To interpret these conflicting results we proposed that the receptors form several subclusters opposite various release sites in presynaptic terminals. This model implies that the release sites operate independently of each other, with no considerable cross-talk between neighboring subclusters. Such a model, of course, has geometrical limitations, depending on the diffusion of transmitter in the synaptic cleft. We therefore calculated concentration profiles of transmitter in the synaptic cleft after the release from a single vesicle. To compare the outcome of such an analysis to experimental results, postsynaptic currents were calculated from the concentration profiles of transmitter using the kinetics of AMPA receptors, but with modified transition rates (Jonas et al., 1993). These currents could then be compared to recorded miniature currents.

Limitations of the model

In recent years attempts have been made to find some of the parameters determining synaptic transmission (Clements et al., 1992; Bruns and Jahn, 1995), but many of them remain poorly defined. The purpose of the analysis of transmitter profiles in the cleft was therefore not to provide definitive values for transmitter concentrations but to determine the range of possible values in the context of a well-defined model. The model presented describes diffusion in a simple cylindrical cleft, with a source function describing transmitter release (Bruns and Jahn, 1995), but in the absence of any drain function simulating binding to receptors or reuptake transporters. This simple model was chosen to render an analytical solution possible. The simplification overestimates the actual concentrations of transmitter in the cleft, particularly for the later phases after release. By estimating the binding of transmitter to receptors, the concentration amplitude of the transmitter will be found to be reduced to 85% of its maximum value. (To estimate the loss in postsynaptic concentration due to binding of transmitter to the receptors, we took into account 1) the time-dependent probability of binding to a receptor, 2) the maximum number of

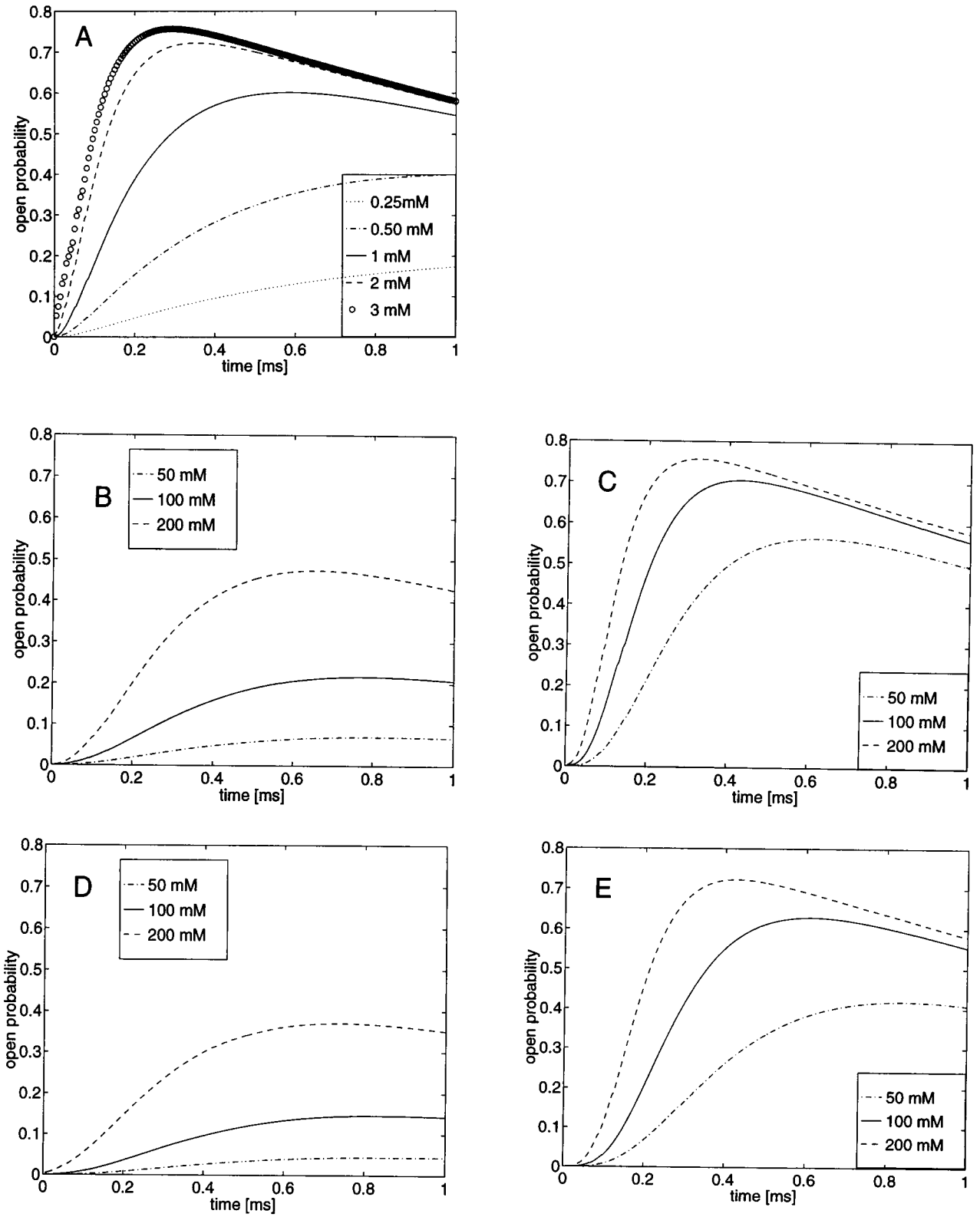

FIGURE 8 Open probability versus time for different transmitter concentrations. (*A*) Stepwise increase to constant transmitter concentrations at the receptors. The open probabilities were calculated for transmitter concentrations from 0.25 mM to 3 mM. (*B–E*) Plots of the open probabilities for calculated postsynaptic transmitter concentrations after α-shaped release from a vesicle containing various initial concentrations from 50 mM to 200 mM. (*B* and *C*) Open probability for $D = 3 \times 10^{-6}$ cm^2/s and $D = 3 \times 10^{-7}$ cm^2/s, respectively, and a radius of a centered receptor field of $r = 50$ nm. (*D* and *E*) Open probability for $D = 3 \times 10^{-6}$ cm^2/s and $D = 3 \times 10^{-7}$ cm^2/s, respectively, and a radius of a centered receptor field of $r = 100$ nm.

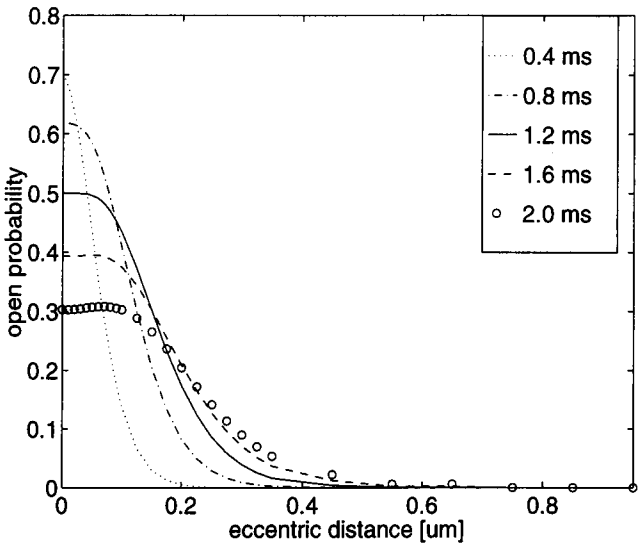

FIGURE 9 Influence of the site of the receptor clusters relative to the site of the release pore on the peak open probability. Channel open probability versus eccentric distance for different times after the onset of α-shaped release. The abscissa is the lateral distance of the patch from the release pore (eccentric distance in μm). The circular membrane patches all have the same radius ($r = r_{cyl} = 50$ nm). $D = 3 \times 10^{-7}$ cm^2/s.

bound molecules in a receptor cluster, 3) the fraction of molecules in the effective volume versus environment, and 4) the fact that a particle sink at the receptor site will be refilled with particles from the environment because of quasi-instantaneous diffusion on a small length scale, <5 nm; see Fig. 6.) The fact, that the modeling of the miniature currents, although producing good fits for the rising phase, was too slow for the decaying phase (cf. Fig. 7 *B*) may be explained by the overestimation of the concentration in this phase. In the long time range an equilibrium is established between binding and unbinding transmitter as long as release is going on. This will lead to a persisting shift of the postsynaptic concentration toward lower values. Because the main purpose of our study was to evaluate cross-talk phenomena between neighboring subclusters of receptors due to rapid lateral diffusion of transmitter, the absence of drain functions is something like the worst case in terms of the spatial separation of two subclusters necessary to avoid cross-talk.

A Gaussian function in space and an α-shaped function in time were used as the source function of transmitter. Because no similar data on glutamate release are available so far, the time course of serotonin release in cultured Retzius cells of the leech was combined with the range of values proposed for the concentration of glutamate in synaptic vesicles and in the cleft (Bruns and Jahn, 1995; Clements et al., 1992). The size and transmitter content of the small transparent vesicles in the leech Retzius cells (mean diameter 38 nm, 4200 molecules) are in the same range as reported for mammalian glutamatergic synapses. It seems reasonable therefore to assume that the release kinetics are also similar. To evaluate our analysis against other approaches (Wathey et al., 1979; Faber et al., 1992; Holmes, 1995; Wahl et al., 1996), instantaneous and continuous release functions were compared. By using instantaneous release functions, results similar to those as reported by the authors mentioned above were obtained, verifying the reliability of the model. However, regarding the time course of transmitter in the cleft, continuous α-shaped release produced concentrations similar to those proposed for glutamate (Clements et al., 1992; Barbour et al., 1994) in synapses of cultured hippocampal cells. With instantaneous release this was not seen (Wathey et al., 1979; Busch and Sakmann, 1990; Khanin et al., 1994; Holmes, 1995; Wahl et al., 1996). The decay of glutamate after instantaneous release is too fast. (For an intermediate release model (cf. Wahl et al., 1996, transmitter diffusing out of the vesicle pore) the concentration profiles were also faster than experimentally observed.) This is a remarkable difference between continuous and instantaneous release. The two sets of kinetic constants proposed by Jonas et al. to fit hippocampal AMPA currents could not be taken unchanged for spinal currents because they predicted currents that were too slow even for a stepwise change to saturating transmitter concentration. Therefore the constants were altered to satisfy the constraints given in the Kinetic Model section above. Under the hypothesis of a saturating glutamate concentration at the postsynaptic side, these constraints could be satisfied with the low diffusion coefficient (3×10^{-7} cm^2/s) only (see Figs. 7 *A*, and 8, *C* and *E*). However, they could not be satisfied when the peak postsynaptic concentration of transmitter was lower due to the "normal" diffusion coefficient. When points 1) to 4) wer satisfied under such conditions, the rise time of the currents was too slow (Figs. 7 *B*, and 8, *B* and *D*). The five constraints also could not be fulfilled when k^*_{ab} was lowered by a factor of 10 (to 4 mM^{-1} ms^{-1}) to account for the proportional change in the diffusion coefficient. However, this is not astonishing, because the rate constant is only proportional to the diffusion coefficient when the reaction is mainly diffusion controlled. It is not necessarily the case for activation-controlled reactions. The low value of k^*_{ab} ($\ll 10^3$ mM^{-1} ms^{-1}) suggests that the binding of the transmitter to the receptor is mainly an activation-controlled process (Atkins, 1994).

Implications for synaptic structure

When a hypothetical diffusion coefficient of glutamate in the cleft ($D = 3 \times 10^{-6}$ cm^2/s) (Wathey et al., 1979; Busch and Sakmann, 1990; Holmes, 1995) is used, the concentration of glutamate at the postsynaptic membrane at the time of the peak current shows a wide lateral distribution (Fig. 5, *A* and *C*), thus making any substructure of postsynaptic receptors functionally useless. Under these circumstances the open probability of the receptors reaches a maximum of 47% after 0.6 ms (see Fig. 8 *B*), with a strong dependence of the open probability on the transmitter content in the vesicle. The high value of D would therefore be in agree-

ment with a model in which postsynaptic receptors are not fully saturated during release, and in which the size of the postsynaptic current (and its variance) is determined by the (variable?) concentration of glutamate in the vesicles or by the (variable?) size of the vesicles. It must be noted, however, that this model predicts slower currents than are actually measured. To achieve full saturation of receptors during release, the concentration of transmitter at the postsynaptic membrane must be increased. This can be achieved in three ways. First, the content of transmitter in the vesicle can be higher than 200 mM. Second, release of transmitter can be driven by other forces in addition to pure diffusion. And third, the diffusion coefficient may be lower than assumed, leading to a reduced lateral spread of transmitter and consequently to a higher concentration of transmitter at the receptors located opposite the release site. Although we cannot exclude the first two possibilities, we consider the last possibility the most likely for the following reasons. The content of glutamate in a vesicle was estimated to be in the range of 60–200 mM (Clements et al., 1992), and we have no reason to question these values. (For physiological reasons the concentration will not exceed the isotonic limit of 300 mM. For concentrations of 200 mM refer to Fig. 8, *B–E* (upper traces).) So far there is no experimental evidence for a mechanism other than diffusion driving the release of transmitter. (To our knowledge there is only one report questioning the assumption that diffusion alone governs transmitter release (Khanin et al., 1994). Their argument is based on the assumption of a very narrow opening of the vesicle.) In contrast, it is reasonable to assume that the diffusion coefficient in the synaptic cleft is lower than expected for pure water, because the cleft is known to contain a fuzzy material, the basal membrane, at least at active zones. This basal membrane could act as a diffusion brake. Because of the narrowness of the cleft, the time the transmitter needs to reach the postsynaptic side is not significantly affected by a lower diffusion coefficient. However, the concentration is higher in a smaller volume because of the lower diffusion rate. A decrease in the diffusion coefficient by a factor of 10 increases the peak open probability to 76% for channels located opposite the release site (cf. Fig. 8, *C* and *E*). Seventy-six percent corresponds to the maximum open probability (79%), which is defined by the channel kinetics and not by the available transmitter (cf. Fig. 7 *C*). The profile of the concentration of transmitter at the postsynaptic membrane under these conditions shows a steep decay within a radius of 50 to 200 nm (see Fig. 5 *B*). Therefore concentrically situated receptors would be saturated for early times ($t < 600$ μs), whereas eccentrically situated receptors outside a radius of 300 nm would be largely unaffected by the transmitter released from one vesicle (cf. Fig. 9). For later times (600 μs $< t <$ 2 ms; see Fig. 9) the significant spillover of transmitter to neighboring clusters is only slightly increased to a radius of 400 nm. This is also probably limited by binding of glutamate to uptake molecules. Under these circumstances, subclustering of receptors would be functionally relevant and could account for the conflicting results mentioned in the Introduction. The variability of miniature currents may be explained in this model by independently operating release sites with receptor clusters of variable sizes in one bouton. It is an open question how such an organization of postsynaptic receptors into functionally relevant subclusters may be related to the active zones. Recent evidence from an ultrastructural study (Baude et al., 1995) suggests that the AMPA receptors are mainly clustered in the postsynaptic densities or active zones. Ultrastructural data of central synapses show a lot of variation, depending on what types of synapses and what species are looked at. In spinal ventral horn of the adult cat, Ia afferent boutons have a mean apposition area of 6.8 μm^2, with the majority of the values laying between 0.2 and 10 μm^2 (Pierce and Mendell, 1993). These synapses show on average six active zones per bouton (most values are between two and eight). In fetal mouse spinal cord cultures, an average apposition area of 1.9 μm^2 and a mean number of two active zones for interneuronal synapses and one large active zone for synapses between sensory neurons and interneurons are reported (Neale et al., 1983). In turtle spinal cord an apposition area of 1.5 μm^2 was found, with 50% of the synapses having more than one (two to four) active zones (Yeow and Peterson, 1991). In all of these examples the geometry of the synapse would be consistent with an independent function of single release sites. The possibility of having several independent release sites in one bouton throws a new light on the release of multiple vesicles in one bouton. Depending on where the second vesicle is released related to the first, their transmitter can interact with the same cluster of postsynaptic receptors (Tong and Jahr, 1994), or it can interact with two separate clusters, causing an increase in the efficacy of the synapse. The model is also consistent with the possibility of the facilitation of transmission at neighboring release sites (Faber and Korn, 1988) due to single binding of ambient glutamate to the receptors, although this has not been shown so far for spinal glutamatergic synapses.

CONCLUSIONS

We have shown that in a plausible model of synaptic release and diffusion in the cleft, saturation of postsynaptic receptors and sufficiently fast postsynaptic currents can only be achieved if the coefficient of diffusion in the cleft is one order of magnitude smaller than in aqueous solution. Under this assumption the lateral width of the transmitter distribution in the cleft is narrow and therefore cross-talk effects between neighboring release sites in a bouton with multiple postsynaptic receptor clusters are minimal. Thus an independent function of multiple release sites in one bouton is possible in the absence of lateral diffusion barriers. This may explain the variability of miniature currents originating from one bouton.

APPENDIX

Homogeneous diffusion equation

Continuous release is described by the inhomogeneous diffusion equation (Eq. 1). In comparison to Eq. 1, it is sufficient for instantaneous release to consider a homogeneous diffusion equation what is done in this section. The inhomogeneous diffusion equation is considered in the next section. An analytical solution for the homogeneous diffusion equation is presented with a Gaussian initial distribution in space. The result will be used as a reference for transmitter concentration profiles after instantaneous release. Let us consider the density n of transmitter molecules. The time evolution of n is given by the homogeneous diffusion equation

$$\frac{\partial}{\partial t} n(x, y, z, t) = D\left(\frac{\partial^2}{\partial x^2} + \frac{\partial^2}{\partial y^2} + \frac{\partial^2}{\partial z^2}\right) n(x, y, z, t). \quad (6)$$

n is a function of time and space variables. To model diffusion without barriers, free boundaries at infinity are chosen. Any solution is determined then by the initial $t_0 \equiv 0$ distribution $n(x, y, z, 0)$.

To model the instantaneous transmitter release we choose a Gaussian initial distribution

$$n(x, y, z, 0) = A \exp\left\{-\left(\frac{x^2 + y^2}{b} + \frac{z^2}{c}\right)\right\},$$

with amplitude A and standard deviation $\sqrt{b}/2$ in the parallel and $\sqrt{c}/2$ in the perpendicular direction (cf. the spatial distribution of the source function for continuous release in Eq. 3).

Respecting initial and boundary conditions, Eq. 6 is solved by

$$n(x, y, z, t) = A\frac{b}{(b + 4Dt)}\sqrt{\frac{c}{(c + 4Dt)}} \exp\left\{-\frac{x^2 + y^2}{b + 4Dt} - \frac{z^2}{c + 4Dt}\right\}. \quad (7)$$

$n(x, y, z, t)$ is a function of three Cartesian spatial dimensions and time. For a point initial distribution the solution is to take $b = c = 0$. The finite initial standard deviation $\sqrt{b}/2 > 0$, $\sqrt{c}/2 > 0$ avoids the singularity at $t = 0$.

To compare our findings to other models based on the diffusion equation describing the release of transmitter, we refer to solutions for other release scenarios given by Carslaw and Jaeger (1959). We started with Cartesian coordinates in three dimensions to give results that were as general as possible (see Diffusion Across the Synaptic Cleft, above). The special solution for a cylindrical cleft and an elliptical source turned out to be a function of two variables only. Assuming spherical symmetry allows a reduction to one dimension. For an initial distribution of transmitter in a sphere of radius a centered at the vesicle origin with amplitude A, the spherical diffusion equation is solved (Carslaw and Jaeger, 1959).

The solution is (with free boundaries at infinity)

$$n(r, t) = \frac{A}{2}\left\{\operatorname{erf}\frac{r + a}{2\sqrt{Dt}} - \operatorname{erf}\frac{r - a}{2\sqrt{Dt}} - \frac{2\sqrt{Dt}}{r\sqrt{\pi}}\left(\exp\left\{-\frac{(r - a)^2}{4Dt}\right\} - \exp\left\{-\frac{(r + a)^2}{4Dt}\right\}\right)\right\}. \quad (8)$$

(The error function is defined by $\operatorname{erf}(x) = 2/\sqrt{\pi}\int_0^x \exp\{-t^2\}dt$.) This diffusing distribution is compared to Eq. 7 in Fig. 4.

Diffusion with source term

The inhomogeneous diffusion equation models the source function $f(x, y, z)$. The solution of Eq. 1 is given by a spatial convolution and time integration of Green's function (see below) with the inhomogeneity $f(\cdot, \cdot, \cdot, \tau)$ at position (x, y, z):

$$n(x, y, z, t) = \int_0^t \int_{-\infty}^{\infty}\int_{-\infty}^{\infty}\int_{-\infty}^{\infty} f(\xi, \upsilon, \zeta, \tau)\left(\frac{1}{4\pi D(t - \tau)}\right)^{3/2} \exp\left\{-\frac{(\xi - x)^2 + (\upsilon - y)^2 + (\zeta - z)^2}{4D(t - \tau)}\right\} d\xi d\upsilon d\zeta d\tau. \quad (9)$$

This strategy of solving the inhomogeneous diffusion equation (Eq. 1) can be applied to every source function with the initial value $n(x, y, z, 0) = 0$. Let us check that Eq. 9 indeed satisfies Eq. 1 with the initial condition. A comparison of the integrand in Eq. 9 with the solution of the homogeneous diffusion equation (Eq. 7) shows that Green's function

$$G(x, y, z; t, 0) = \left(\frac{1}{4\pi Dt}\right)^{3/2} \exp\left\{-\frac{x^2 + y^2 + z^2}{4Dt}\right\}$$

is a solution of the homogeneous diffusion equation. Obviously the initial condition $n(x, y, z, 0) = 0$ is fulfilled. To check that Eq. 9 is a solution of Eq. 1, we must differentiate Eq. 9. The time derivation of the upper integration limit converges to the source $f(x, y, z, t)$, so that Eq. 9 solves the inhomogeneous diffusion equation (Eq. 1), obeying free boundary conditions at infinity.

To compare the distribution after α-shaped release in Eq. 3, we refer to a distribution after constant emitting release. The source is emitting transmitter molecules at a constant rate J at the vesicle pore. The position of the source is indicated by the delta function $\delta(x, y, z)$. The initial condition is $n(x, y, z, 0) = 0$. The corresponding spherical inhomogeneous diffusion equation is solved (cf. Carslaw and Jaeger, 1959) by the complementary error function, erfc,

$$n(r, t) = \frac{J}{4\pi Dr} \operatorname{erfc}\frac{r}{\sqrt{4Dt}}, \quad (10)$$

where $\operatorname{erfc}(x) = 1 - \operatorname{erf}(x)$. It turns out that Eq. 10 is a function of the Euclidean distance $r = \sqrt{x^2 + y^2 + z^2}$ and time. This is the simplest noninstantaneous source one can assume. In Fig. 4 postsynaptic transmitter concentration versus time for continuous and α-shaped release is compared to instantaneous release. The densities $n(x, y, z, t)$ rsp $n(r, t)$ must be modified according to the cleft geometry, applying the procedure in the next section. The transformation into postsynaptic concentrations is presented under Postsynaptic Concentrations, below.

Diffusion in the synaptic cleft

In the synaptic cleft, the transmitter is reflected at the pre- and postsynaptic sides. The boundary conditions tell us that the derivative in the z direction has to vanish (Neumann boundary conditions at $z = 0$ and $z = d$),

$$\left.\frac{\partial n}{\partial z}\right|_{z=0} = 0 \qquad \left.\frac{\partial n}{\partial z}\right|_{z=d} = 0. \quad (11)$$

This is achieved by the method of reflection. To guarantee that the right equation in Eq. 11 holds, we set another distribution symmetrically to the postsynaptic plane, which satisfies the same dynamics at position $z = 2d$. The particles leaving the region $0 \le z \le d$ are replaced by those entering from the region $d \le z \le 2d$, so that the gradient at $z = d$ equals zero. This violates the boundary condition in Eq. 11 at $z = 0$. To satisfy the condition of the left-hand side, we introduce a third distribution centered at $z = -2d$, and so on. Affiliating all sources in a chain at positions $z = 2jd$ for any integer j leads to Eq. 2.

Equation 2 solves Eq. 1 inside the cleft with the initial condition $n(x, y, z, t) = 0$ and boundary condition Eq. 11. The boundaries in the x and y directions are still free. Each summand in Eq. 2 is finite. For the interesting time range ($0 < t < 1$ ms) and range of D, it is sufficient to use the central 20 summands, because the contributions of the summands decline rapidly with distance z. With increasing time more terms corresponding to a greater distance contribute significantly to the result. The solution of Eq. 2 is an analytical result. Any source function $f(\xi, \upsilon, \zeta, \tau)$ may be inserted into the integrand. In contrast to Eq. 9, Eq. 2 takes into account the accumulation (by the Neumann boundary condition) of particles at the pre- and postsynaptic membranes. By inserting the source term as given in Eqs. 3 and 4 in Eq. 2, the space integrals are solvable. Integrating over the space variables in Eq. 2 and substituting $s = 4D(t - \tau)$, we get Eq. 5. (The procedure is identical for x, y, and z. After completing the square in the exponent term, one makes use of the integral $\int_{-\infty}^{\infty} \exp\{-\alpha x^2\}\, dx = \sqrt{(\pi/\alpha)}$.)

The two spatial variables x and y are replaced by r to take the cylinder symmetry of the problem into account. In this coordinate frame the diffusion process can be treated as two-dimensional in space (cf. Fig. 2 *A*).

The integral of $f(x, y, z, t)$ over the cleft (space) and time equals to the amount Q of transmitter contained in one vesicle:

$$\int_{\text{space}} \int_{\text{time}} f(x, y, z, t)\mathrm{d}t\mathrm{d}x\mathrm{d}y\mathrm{d}z \tag{12}$$
$$= q\pi^{3/2} b \sqrt{c} \int_{\text{time}} t^{\alpha}\exp\{-\beta t\}\mathrm{d}t \overset{!}{=} Q.$$

Equation 12 determines the normalization constant q = molecules/(μm^3 μs$^{5/4}$) calculated for $Q = 2000$ molecules. Integrating Eq. 5 over z and r, one gets a sum of sources $\Sigma_{j=-\infty}^{\infty} Q_j$ analogous to Eq. 12. Within the synaptic cleft, this means that the integral over the distribution equals the amount of transmitter set free from the vesicle (no particle sources or sinks).

Postsynaptic concentrations

To reconstruct postsynaptic currents and to compare them to experimentally recorded currents, the concentration of transmitter at the postsynaptic membrane must be calculated. For a circular patch of postsynaptic membrane with a given radius r_{cyl}, the transmitter densities (Eq. 5) can be transformed into concentrations as follows. One must specify the radius of the patch r_{cyl} and the height h of the transmitter cylinder interacting with the receptors (cf. Fig. 2 *A*). (By the uniformity of the transmitter density over the cleft width (cf. Fig. 6), the numerical value of h is of minor importance.). Integrating the density according to Eq. 5 from $r = 0$ to $r = r_{cyl}$ and from $z = d - h$ to $z = d$, one gets the amount of transmitter in front of the chosen membrane patch. The amount of transmitter in the cleft is calculated by integrating Eq. 5 from $r = 0$ to $r = \infty$ and from $z = 0$ to $z = d$. The ratio of the two integrals ($\text{ratio}_{\text{cleft}}$) gives the number of transmitter molecules in front of the receptors relative to that in the cleft,

$$\text{ratio}_{\text{cleft}}(r_{cyl}, h, t) = \int_{d-h}^{d} \int_{0}^{r_{cyl}} n(r, z, t) r\mathrm{d}r\mathrm{d}z \Big/ \int_{0}^{d} \int_{0}^{\infty} n(r, z, t) r\mathrm{d}r\mathrm{d}z.$$

Up to time t, the source released a fraction

$$\text{ratio}_{\text{source}}(t) = \int_{0}^{t} \tau^{\alpha}\exp\{-\beta\tau\}\mathrm{d}\tau \Big/ \int_{0}^{\infty} \tau^{\alpha}\exp\{-\beta\tau\}\mathrm{d}\tau.$$

The volume ratio is

$$\text{ratio}_{\text{volume}}(r_{cyl}, h) = V_{ves}/V_{cyl} = 4r_{ves}^3/3h \cdot r_{cyl}^2.$$

Multiplying the three ratios and the initial concentration c_0 in the vesicle gives the postsynaptic concentration at time t ($\text{conc}_{\text{rec}}(t)$) averaged over the membrane patch:

$$\text{conc}_{\text{rec}}(r_{cyl}, h, t) \tag{13}$$
$$= \text{ratio}_{\text{cleft}}(r_{cyl}, h, t) \cdot \text{ratio}_{\text{source}}(t) \cdot \text{ratio}_{\text{volume}}(r_{cyl}, h) \cdot c_0.$$

We thank Christoph Amstutz for helpful discussion and Matthew Larkum and Dr. Alexander Dityatev for critical readings of the manuscript.

This work was supported by grants from the Swiss National Science Foundation, 31-39419.93 (JS), 3100-042055.94 (HRL), and 5002-037939 (HRL and LM). The mathematical implementation of the model is available at http://iamwww.unibe.ch/~brainwww/.

REFERENCES

Atkins, P. W. 1994. Physical Chemistry. Oxford University Press, Oxford, Melbourne, Tokyo.

Baude, A., Z. Nusser, E. Molnar, R. A. J. McIlhinney, and P. Somogyi. 1995. High-resolution immunogold localization of AMPA type glutamate receptor subunits at synaptic and non-synaptic sites in rat hippocampus. *Neuroscience.* 69:1031–1055.

Barbour, B., B. U. Keller, I. Llano, and A. Marty. 1994. Prolonged presence of glutamate during excitatory synaptic transmission to cerebellar Purkinje cells. *Neuron.* 12:1331–1343.

Bartol, T. M. Jr., B. R. Land, E. E. Salpeter, and M. M. Salpeter. 1991. Monte Carlo simulation of miniature endplate current generation in thevertebrate neuromuscular junction. *Biophys. J.* 59:1290–1307.

Bekkers, J. M., G. B. Richerson, and C. F. Stevens. 1990. Origin of variability in quantal size in cultured hippocampal neurons and hippocampal slices. *Proc. Natl. Acad. Sci. USA.* 87:5359–5362.

Bruns, D., and R. Jahn. 1995. Real time measurement of transmitter release from single synaptic vesicles. *Nature.* 377:62–65.

Busch, C., and B. Sakmann. 1990. Synaptic transmission in hippocampal neurons: numerical reconstruction of quantal IPSCs. *Cold Spring Harb. Symp. Quant. Biol.* 55:69–80.

Carslaw, H. S., and J. C. Jaeger. 1959. Conduction of Heat in Solids, 2nd Ed. Oxford University Press, New York.

Clamann, H. P., Rioult, M. S. Pedotti, and H.-R. Lüscher. 1991. The influence of noise on quantal EPSP size obtained by deconvolution in spinal motoneurons in the cat. *J. Neurophysiol.* 65:67–75.

Clements, J. D., R. A. J. Lester, G. Tong, C. E. Jahr, and G. L. Westbrook. 1992. The time course of glutamate in the synaptic cleft. *Science.* 258:1498–1502.

Colquhoun, D., P. Jonas, and B. Sakmann. 1992. Action of brief pulses of glutamate on AMPA/kainate receptors inpatches from different neurones of rat hippocampal slices. *J. Physiol. (Lond.).* 458:261–287.

Del Castillo, J., and B. Katz. 1954. Quantal components of the end-plate potential. *J. Physiol. (Lond.).* 124:560–573.

Dityatev, A. E., and H. P. Clamann. 1993. Limits of quantal analysis reliability—quantal and unimodal constraints and setting of confidence intervals for quantal size. *J. Neurosci. Methods.* 50:67–82.

Faber, D. S., and H. Korn. 1988. Synergism at central synapses due to lateral diffusion of transmitter. *Proc. Natl. Acad. Sci. USA.* 85: 8708–8712.

Faber, D. S., W. S. Young, P. Legendre, and H. Korn. 1992. Intrinsic quantal variability due to stochastic properties of receptor-transmitter interactions. *Science.* 258:1494–1498.

Holmes, W. R. 1995. Modeling the effect of glutamate diffusion and uptake on NMDA and non-NMDA receptor saturation. *Biophys. J.* 69:1734–1747.

Isaacson, J. S., and B. Walmsley. 1995. Counting quanta: direct measurements of transmitter release at acentral synapse. *Neuron.* 15:875–884.

Jonas, P., G. Major, and B. Sakmann. 1993. Quantal components of unitary EPSCs at the mossy fibre synapse on CA3 pyramidal cells of rat hippocampus. *J. Physiol. (Lond.).* 472:615–663.

Khanin, R., H. Parnas, and L. Segel. 1994. Diffusion cannot govern the discharge of neurotransmitter in fast synapses. *Biophys. J.* 67:966–972.

Kullmann, D. M., and R. A. Nicoll. 1992. Long-term potentiation is associated with increases in quantal content. *Nature.* 357:240–244.

Larkman, A., K. Stratford, and J. Jack. 1991. Quantal analysis of excitatory synaptic action and depression in hippocampal slices. *Nature.* 350: 344–347.

Liu, G., and R. W. Tsien. 1995. Properties of synaptic transmission at single hippocampal synaptic boutons. *Nature.* 375:404–408.

Longsworth, L. G. 1953. Diffusion measurements at 25°, of aqueous solutions of amino acids, peptides and sugars. *J. Am. Chem. Soc.* 75:5705–5709.

Malinow, R., and R. W. Tsien. 1990. Presynaptic enhancement shown by whole cell recordings of long-term potentiation in hippocampal slices. *Nature.* 346:177–180.

MathWorks. MATLAB(R), Version 4.2c. The MathWorks, Natick, MA.

Neale, E. A., P. G. Nelson, R. L. MacDonald, C. N. Christian, and L. M. Bowers. 1983. Synaptic interactions between mammalian central neurons in cell culture. III. Morphophysiological correlates of quantal synaptic transmission. *J. Neurophysiol.* 49:1459–1468.

Pierce, J. P., and L. M. Mendell. 1993. Quantitative ultrastructure of Ia boutons in the ventral horn: scaling and positional relationships. *J. Neurosci.* 13:4748–4763.

Redman, S. 1990. Quantal analysis of synaptic potentials in neurons of the central nervous system. *Physiol. Rev.* 70:165–198.

Smirnow, W. I. 1958a. Lehrgang der hoeheren Mathematik II, 12th Ed. VEB Deutscher Verlag der Wissenschaften, Berlin.

Smirnow, W. I. 1958b. Lehrgang der hoeheren Mathematik V, 12th Ed. VEB Deutscher Verlag der Wissenschaften, Berlin.

Tang, C.-M., M. Margulis, Q.-Y. Shi, and A. Fielding. 1994. Saturation of postsynaptic glutamate receptors after quantal release of transmitter. *Neuron.* 13:1385–1393.

Tong, G., and C. E. Jahr. 1994. Multivesicular release from excitatory synapses of cultured hippocampal neurons. *Neuron.* 12:51–59.

Trussell, L. O., and G. D. Fischbach. 1989. Glutamate receptor desensitization and its role in synaptic transmission. *Neuron.* 3:209–218.

Vogt, K., H.-R. Lüscher, and J. Streit. 1995. Analysis of synaptic transmission at single identified boutons on rat spinal neurons in culture. *Pflügers Arch.* 430:1022–1028.

Wahl, L. M., C. Pouzat, and K. J. Stratford. 1996. Monte Carlo simulation of fast excitatory synaptic transmission at a hippocampal synapse. *J. Neurophysiol.* 75:597–608.

Wathey, J. C., M. M. Nass, and H. A. Lester. 1979. Numerical reconstruction of the quantal event at nicotinic synapses. *Biophys. J.* 27:145–164.

Wolfram Research. 1994. Mathematica, Version 2.2. Wolfram Research, Champaign, IL.

Yeow, M. B. L., and E. H. Peterson. 1991. Active zone organization and vesicle content scale with bouton size at a vertebrate central synapse. *J. Comp. Neurol.* 307:475–486.